Journal of Structural Geology, Vol. 10, No. 5, pp. 453 to 462, 1988
Printed in Great Britain

0191-8141/88 $03.00 + 0.00

Geometry and tectonic significance of Albian sedimentary dykes in the Sisteron area, SE France

QIN HUANG*

Département de Géotectonique, Université Pierre & Marie Curie, 4 place Jussieu, 75252 Paris 05, France

(*Received* 30 *August* 1987; *accepted in revised form* 17 *February* 1988)

Abstract—Sedimentary dykes in the Sisteron area have penetrated pre-existing fracture sets in late Aptian and early Albian strata. Dynamic characteristics of such fractures are revealed by the bifurcation and the branching of dykes. Three-dimensional statistical analysis of the initial orientation of two vertical conjugate sets of dykes indicates their mechanics of formation, as well as the principal compressional stress direction during the development of the sill–dyke regime in the Sisteron area. Another set of sandstone dykes present in the area suggests syn-sedimentary and extensional faulting tectonic activity before the area became involved in compressional tectonics. Several significant dyke-forms clearly show the sense of shear along fractures filled with sand, and enable the stress pattern during dyke formation in the area to be recognized.

INTRODUCTION

THE association of clastic dykes and sills in turbiditic and argillaceous rocks deposited on submarine slopes is generally attributed to high instability of packed sandstones saturated with water expelled from adjacent shales or muds (Diller 1890, Newson 1903, Jenkins 1952, Truswell 1972, Hiscott 1979). Triggered perhaps by seismic activity (Diller 1890, Pavlow 1896, Duncan 1964, Truswell 1972) or by slumping activities in younger strata (Dzulynski & Radomski 1956), liquified sands penetrate a pre-existing fracture system, forming clastic discordant dykes and concordant sills. Such fracture systems have been examined by several workers (Diller 1890, Newson 1903, Hayashi 1966, Truswell 1972, Beaudoin & Fries 1982) and have been explained as: (1) joint systems triggered by seismic activity (Diller 1890, Pavlow 1896); (2) pre-existing joints in sedimentary strata (Cook & Johnson 1970, Truswell 1972); (3) fault systems related to tectonic deformation and other causes such as hydraulic fracturing (Duncan 1964, Hayashi 1966, Beaudoin & Fries 1982).

Whatever their origin, clastic dykes are clearly associated with fracture systems. Thus, a detailed study of the shape, the spatial distribution and the orientation of dykes in a region may reveal the nature of the tectonic regime prevailing when the dykes were intruded. This paper describes such data for a system of dykes in the Sisteron area, SE France. Based on these data, the stress pattern during sand intrusion is reconstructed and the tectonics of faulting at that time are discussed.

GEOLOGICAL ENVIRONMENT AND DISTRIBUTION OF THE DYKES

Sisteron lies in the E–W-trending Bevons Syncline (Fig. 1). This is in thrust contact to the south with strata underlying Lure Mountain ("Montagne de Lure" in French), which lay on the submarine slope of the Vocontian Basin during the early Cretaceous (Ferry & Flandrin 1979) (Fig. 1). Folds trending E–W were formed during the late Cretaceous and the early Tertiary due to N–S compression affecting the European platform at that time (Bergerat 1987). The most important discordance in the Mesozoic and Tertiary series occurs between the late Cretaceous and the Miocene. In the centre of the syncline, Jurassic and Cretaceous limestones with interbedded shales, several centimetres to several metres thick, form a series of low hills. Aptian and Albian shales with interbedded limestones, approximately 250 m in thickness with well-developed mud slumps, were deposited under 1000–2000 m of water (Fries 1986) and covered by a thick (more than 250 m) marly sequence of late Cretaceous age. Several slump units have been identified. A detailed study of paleocurrent indicators, such as flute casts, reveals that the general current direction in the southern flank of the Bevons Syncline was towards the NE (Beaudoin *et al.* 1983), and slump folds are generally overturned towards the NNE. In the northern flank, however, some sedimentary features, such as traces of lineation due to the motion of sediments on bedding planes in the Bedoulian (Aptian) limestones, show the opposite current direction. During the late Mesozoic, the Sisteron region apparently had a low submarine topographic relief, such as hollows at the base of continental slope (Fries 1986).

In the late Albian, a single turbidite layer, 10–15 m thick and derived from the south, was deposited conformably in the centre of the Bevons Syncline (Fig. 2) (Fries 1986). Beneath the turbidite layer, and derived from it, abundant clastic dykes cut through 200–250 m of late Aptian and early Albian strata, almost reaching the top of the Barremo–Bedoulian (Aptian) limestone beds. Beaudoin & Fries (1982) considered that this downward intrusion of clastic sediments occurred in the late Albian.

The dykes crop out over about 5 km^2 at the northern margin of the syncline, mainly near the village of Bevons

*Present address: 505 Yokoyama Mansion, Honkomagome 3-1-8, Bunkyo-Ku, Tokyo, 113 Japan.

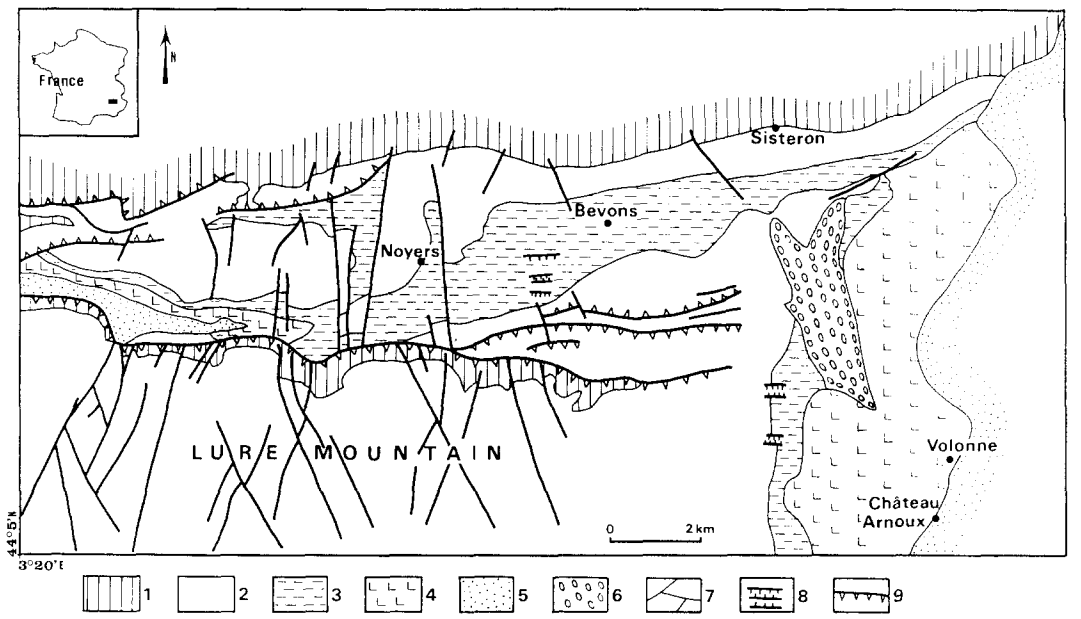

Fig. 1. Geological map of the Sisteron area. 1, Tithonian limestone; 2, limestone with marly interbeds from Beriasian to Aptian; 3, late Aptian to Albian marly limestone; 4, late Albian to Turonian marly limestone; 5, post-Miocene strata; 6, Quaternary alluvial deposits; 7, fault systems; 8, graben–horst system; 9, thrust contacts.

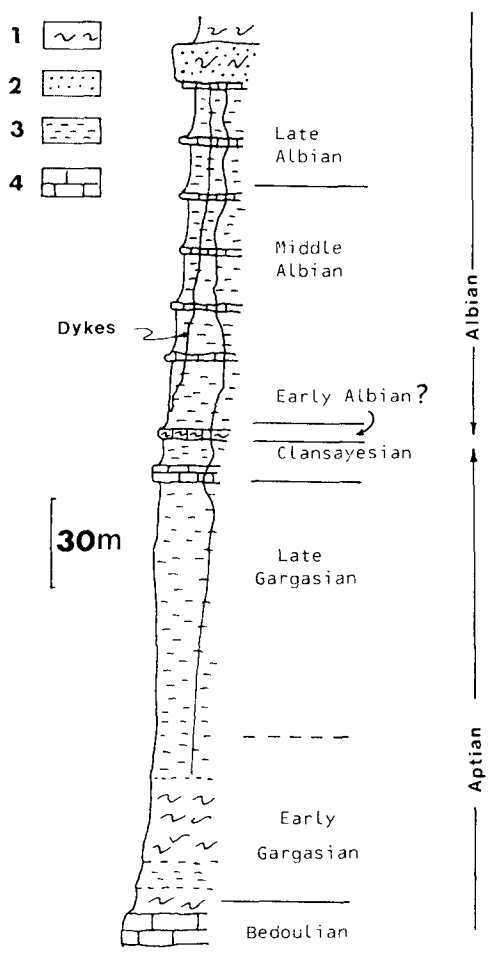

Fig. 2. Stratigraphical sequence of the Aptian and Albian strata in the Sisteron area including the dyke system (from Fries 1986). "Bedoulian" and "Gargasian" are the local sub-stage names referring to limestone with thin marly interbeds in Aptian strata and marly limestone in the late Aptian, respectively (Fries 1986).

(Fig. 3). The occurrence of sandstone dyke systems have been reported in other area of the Vocontian (Rutten & Schonenberger 1957, Beaudoin *et al.* 1983), but no dyke has been found in strata of the same age in nearby regions north and south of the Bevons Syncline.

Immediately above the turbidite, a sequence of slumped marls and some thin (less than 1 m) sandstone beds have been identified (Fries 1986), but the slumping died out gradually from the late Albian to the end of the Mesozoic.

GENERAL DESCRIPTION OF DYKES AND SILLS

In sharp contact with sub-horizontal calcareous and marly beds below the turbidite, the clastic dykes are vertical and essentially tabular with, locally, several branches (Fig. 4c). Their thickness decreases gradually downwards but remains horizontally very stable. In an outcrop near Bevons village, the dykes show direct contact with the overlying turbidite source bed. The total range of thickness of the dykes goes from a few millimetres to 150 cm, but most of them are 10–20 cm thick. Although their trace length is more difficult to estimate because of the lack of continuous outcrops, some of the dykes may be over 1 km in length. In some cases, dykes with different orientations may occur together. Where such dykes intersect, they do not offset one another, and they are parallel to joint systems in the adjacent strata.

Clastic sills are generally concordant with adjacent strata. In some cases, the sills transgress from one horizon to another to form a dyke–sill system. The areal extent of sills may exceed 1 km^2 and their thickness ranges from a few centimetres to about 2 m. Sills are

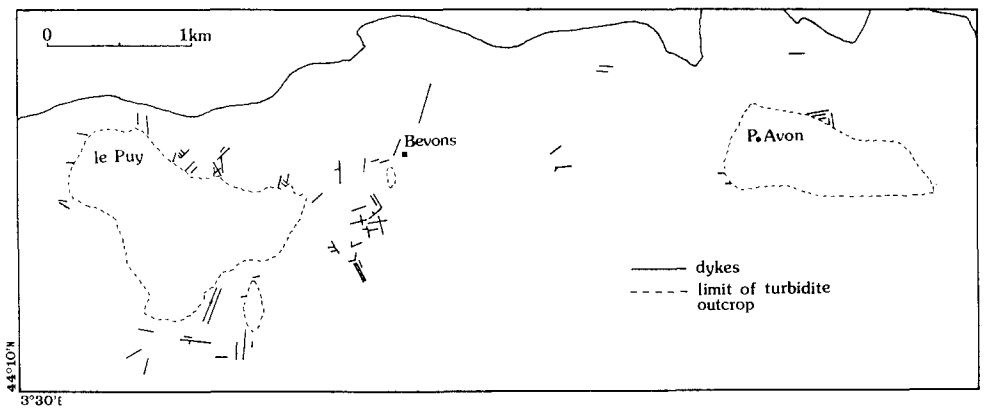

Fig. 3. General distribution of major dykes near Bevons village.

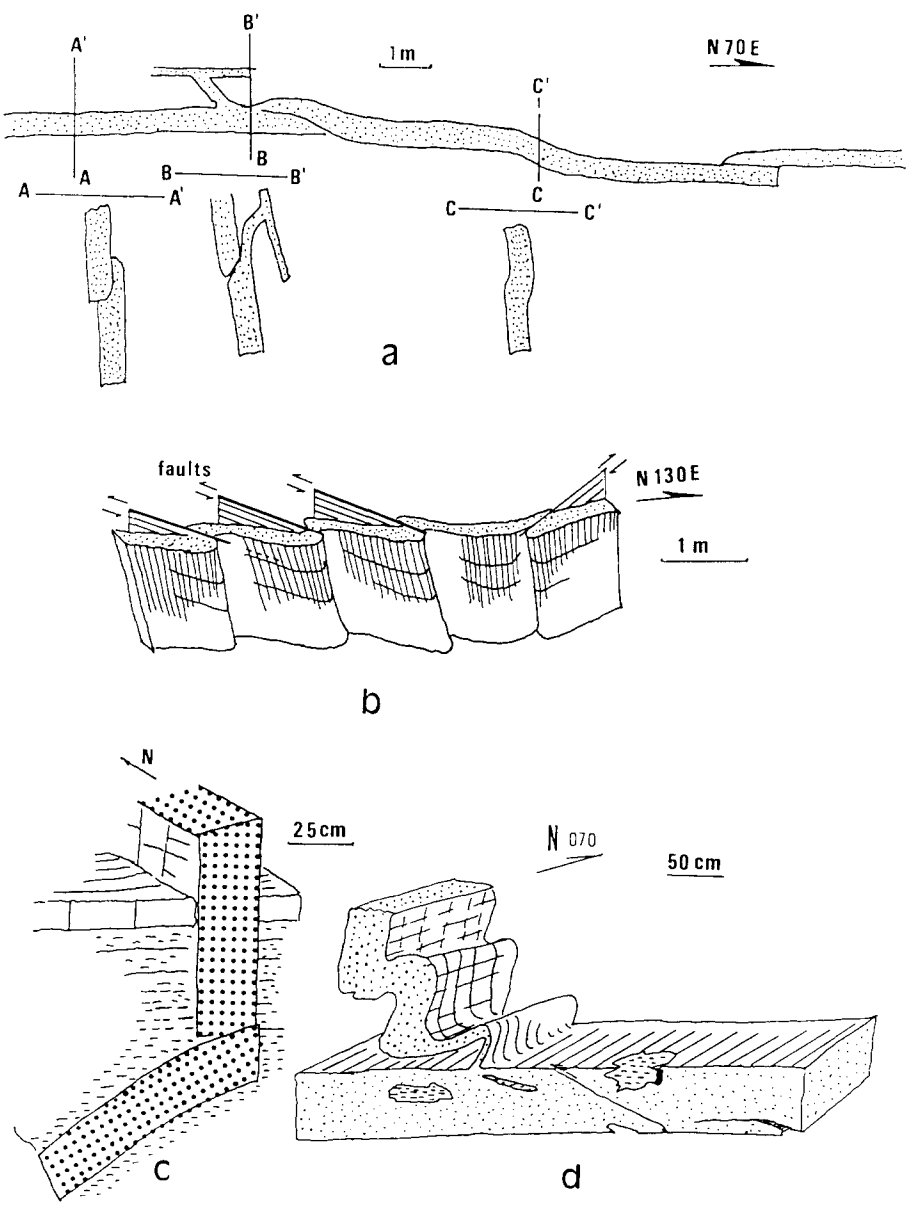

Fig. 4. Several examples of dyke forms. (a) Map view of overlapping form, three vertical sections through the dyke are shown (observed near Pierre-Avon); (b) folds due to tectonic deformation (near Pécoule); (c) abrupt change in dyke orientation caused by the initial orientation of different fractures (near la Baume); (d) contact of dyke with sill (near Bevons); the wavy form of the dyke is due to late diagenetic compaction.

sometimes cut by dykes; in such cases, the sill ends against the dyke or changes its stratigraphical horizon. Microscopic analysis shows that the dykes, sills and the turbidite source have the same petrographic composition; clastic dykes are yellow and composed of well-sorted quartz grains which are surrounded by a calcite matrix. The dykes generally exhibit two orthogonal sets of fractures that are perpendicular to the dyke plane; and the density of fractures is inversely proportional to the dyke thickness.

Late compaction of surrounding rocks has resulted in short wavelength folds with horizontal or sub-horizontal axial planes. This occurs near the turbidite source bed, where the amount of compaction is greater than in rocks far below it. Figure 4(d) shows an example of folds caused by the late compaction. The dykes have also undergone many phases of regional tectonic deformation. As shown in Fig. 4(b), the dyke was affected by vertical folds and vertical strike-slip faults; the wavelengths of these folds are generally proportional to the dyke thickness.

It is important to distinguish between the initial and final shape of a dyke. Only the initial shape can be considered as an indicator of the characteristics of fractures at the time of intrusion (Duncan 1964, Hayashi 1966, Symers & Peterson 1971). The final shape may only be used to analyze the compaction effects and late tectonic deformations (Hiscott 1979).

STATISTICAL ANALYSIS OF THE DYKE SYSTEM

Taking the statistics of orientation data as a tool (e.g. Mardia 1972), a statistical analysis on dyke orientation, combined with a large-scale study of the fracture systems in the same region, was carried out to establish the relationship between regional geological phenomena such as faulting and the mechanism of sedimentary dyke formation. Duncan (1964) demonstrated that the fracture system associated with the clastic dykes in California was intimately related to the regional history of fracturing. Hayashi (1966) stated that such fractures were probably the result of tectonic events. Based on the orientation data of dyke planes, the statistical analysis is aimed at establishing the possible correlation between orientations of dyke planes and fracture sets in their vicinity.

Considering that there was no significant large-scale regional deformation before the late Albian (Ferry & Flandrin 1979), bedding in the Bevons region was approximately horizontal at the time of intrusion. To restore each dyke to its original orientation, the actual data should be rotated about the strike of bedding through an angle equal to the dip of bedding. Using 107 measurements of dyke orientation data as illustrated in Fig. 5 (each datum representing the orientation of a dyke) and applying the contouring technique to the data set after stratigraphic correction for each dyke (Huang *et al.* 1987), three sets of measurements of dyke orientation have been distinguished (Fig. 5c). For the purpose of statistical analysis, the dynamical cluster procedure proposed by Diday (1971) was adapted to isolate these three sets and illustrate them separately in Fig. 6. A specific name was given to each set: Sets 1, 2 and 3 have mean strikes of N003°E (Fig. 6a), N070°E (Fig. 6b) and N135°E (Fig. 6c), respectively. Based on spherical statistics (Fisher 1953, Watson 1960, 1965, Mardia 1972) the characteristics and the statistical parameters (see definitions in the Appendix) of each set are summarized in Table 1, from which it is easy to see that Sets 1 and 2 were initially perpendicular to bedding, whereas Set 3 dipped steeply towards the SW. Among the three sets, Set 1 is most tightly distributed around the preferred axis while Set 3 is rather dispersed and some elements of Set 3 are close to the other two sets (Fig. 5a); Set 2 is the major set with 44 dykes (41.1% of the data set) and Set 3 is the minor one with only 28 dykes (26.6%).

According to Borradaile (1984), sedimentary dykes formed by forced sand injection in fissures are generally perpendicular to the bedding. However, several cases with different orientations have already been described (Cross 1894, Pavlow 1896), so that perpendicularity is

Table 1. Statistical parameters of three sets of dykes

	Set 1			Set 2			Set 3		
Total number	35			44			28		
Orientation matrix	30.6	−1.4	2.90	7	0.34	0.10	11.7	10	−4.7
		3.1	0.04		33.7	−0.01		12	−4.8
			1.30			3.20			4.2
Eigenvectors τ_1	0.99	−0.05	0.10	−0.3	0.9	−0.02	0.67	0.67	−0.30
τ_2	0.04	0.99	0.05	−0.1	−0.01	0.99	0.50	−0.10	0.85
τ_3	−0.1	−0.04	0.99	0.9	0.3	0.08	0.50	−0.70	−0.40
Eigenvalues λ_1	31			38.1			24.3		
λ_2	3			3.2			1.9		
λ_3	1			2.7			1.8		
$\varkappa$	9			8.4			7.8		
Φ	2.04			13.3			25.77		
Preferred plane	N003°E 84E			N70°E 90			N135°E 72SW		
Cluster form	Axial			Axial			Axial		

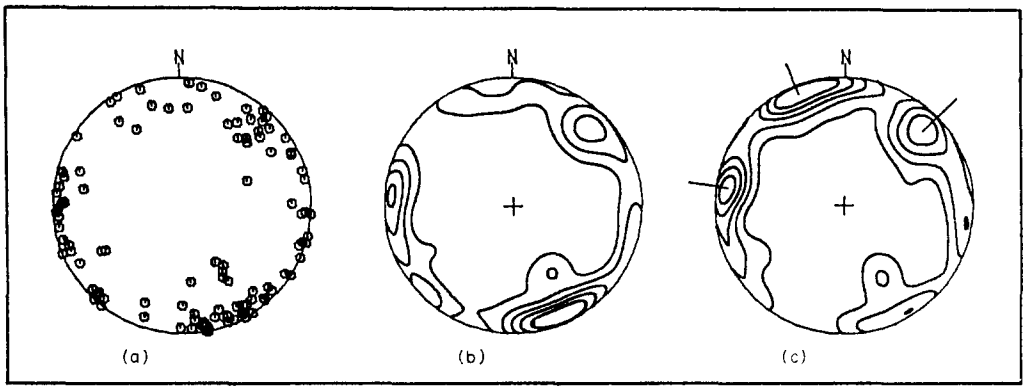

Fig. 5. Equal-area projection (lower hemisphere) of 107 dykes. (a) All poles without stratigraphic correction; (b) contour diagram with $k = 40$ (at levels of 90, 80 , 70, 60 and 50%, normalized with the maximum density within the population (see Huang *et al.* 1987); (c) contour diagram of the data after stratigraphic correction with $k = 40$ at the same levels as in (b).

not verified everywhere. As shown in Fig. 6, the dykes in the Sisteron area are unusual since those of Set 3 do not appear to be vertical. This is indeed the case proven by some statistical tests aimed at verifying the verticality of all dyke planes. The null hypothesis is formed to verify the perpendicularity between the dyke planes and the general bedding (supposed to be horizontal at the time of intrusion): taking the vertical unit vector $S(0, 0, 1)$ as the normal to the bedding, the null hypothesis H_0 is $S = \tau$, where τ is the vector around which the moment of inertia is minimum if we assign unit mass to each pole of the dykes. If τ lies within the confidence cone associated with their distribution, the null hypothesis cannot be rejected. The test is to verify the following relation given by Mardia (1972, p. 279)

$$S.T.S' < a = \lambda_3(n - 2 + F(\alpha)_{2,n-2})/(n - 2),$$

where T is the orientation matrix (see Appendix), λ_3 is

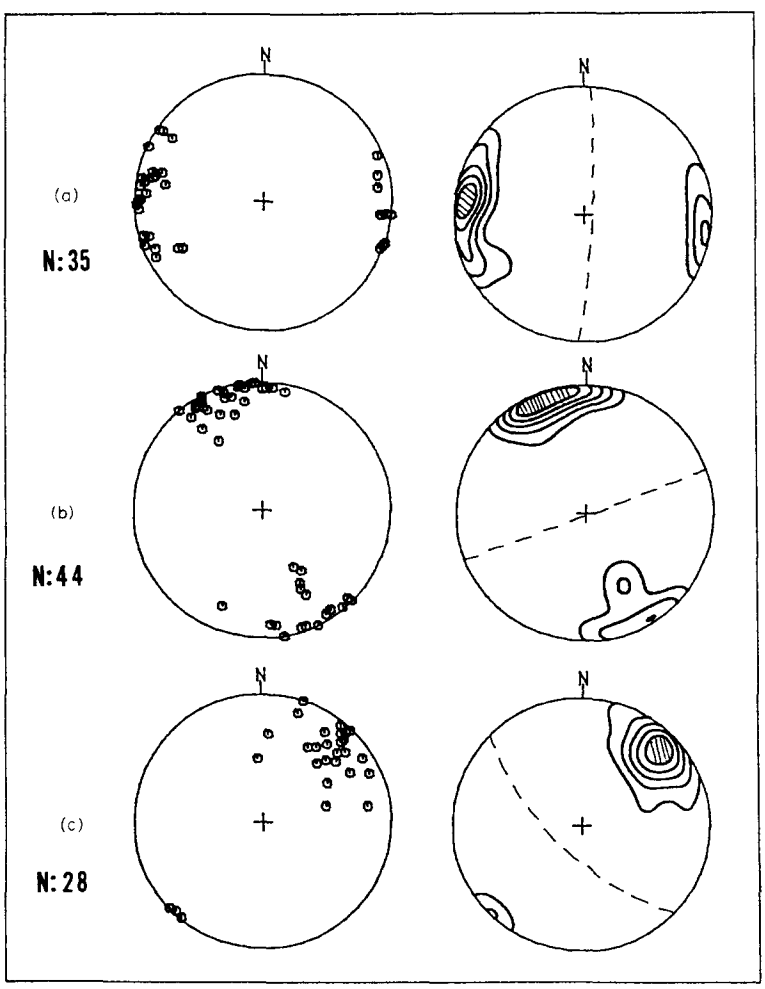

Fig. 6. Equal-area projection (lower hemisphere) of the three sets of dykes. The left-hand column shows all poles of dykes, the right-hand column shows contour diagrams (identical legend to that in Fig. 5) and the preferred plane of each set (dotted line).

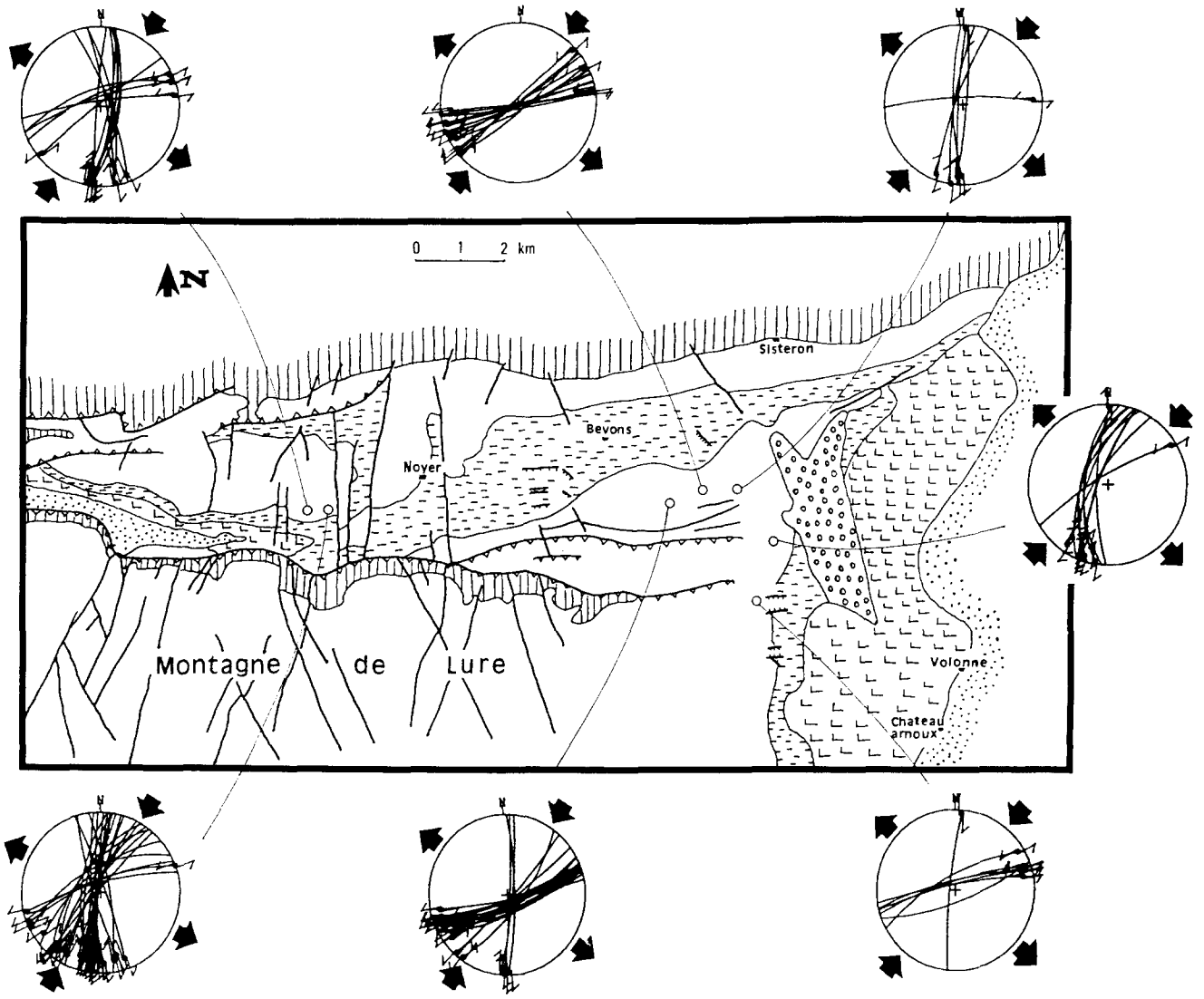

Fig. 7. Strike-slip faults, direction of compressional and extensional stresses and locality of sampling. Micro-fault data are shown by the fault planes and orientation of striae on faults. The stress pattern, associated with faults in each site, is reconstructed by using the method of Huang & Angelier (1987), and the directions of compressional and extensional stresses are shown by the black arrows. Dextral and sinistral faults trend approximately N–S and N070–080°E, respectively; both sets are perpendicular to bedding. The calculated direction of compressional stress is about N030–040°E. The stratigraphic units are the same as in Fig. 1. The diagrams are lower hemisphere equal-area projections.

the smallest eigenvalue of $\boldsymbol{T}$, $F(\alpha)$ corresponds to the F distribution with 2 and $n-2$ degrees of freedom at level α, and n is the total number of dykes in the data set for which the test of the null hypothesis is carried out.

The first test was carried out using all 107 dykes with $\alpha = 0.05, \lambda_3 = 7.9, F(\alpha)_{2,105} = 3.08$ and their orientation matrix. This gives $\boldsymbol{S}.\boldsymbol{T}.\boldsymbol{S}' = 8.75 > a = 8.37$, so the null hypothesis is rejected. The data are not all perpendicular to the bedding. The second statistical test concerns a mixed population of the dykes belonging to Sets 1 and 2. The total number is 79, $\lambda_3 = 4.2$, $F(\alpha)_{2,77} = 3.1$ and $\boldsymbol{S}.\boldsymbol{T}.\boldsymbol{S}' = 4.526 < a = 4.538$. Thus, the hypothesis of perpendicularity of this mixed population is accepted. Consequently, one can be assured that within the total population, there are two sets forming a sub-population (Sets 1 and 2) that is perpendicular to the general bedding at the time of intrusion.

Analyses of joint systems in Aptian and early Albian strata have revealed two sets of well-developed joints which trend N–S and N070°E, respectively, and both are perpendicular to the general bedding (Huang 1987). Consequently, there is a possible orientational correlation between these joints and some of the dykes. For the purpose of reconstructing the paleostress pattern, a study of micro-faults has also been carried out. Measurements (orientation of planes, striae) in Aptian limestone beds have revealed two sets of conjugate faults which trend approximately N–S (dextral) and N070°E (sinistral) (Fig. 7). These faults have not been observed in the strata younger than late Albian. The dykes of Sets 1 and 2 are clearly parallel to these conjugate faults. One can reasonably assume that the dykes of Sets 1 and 2 may have used two sets of conjugate fractures. Moreover, some normal faults, oriented near N130–140°E with small offset of beds, have been observed in the late Aptian limestone beds. These faults are parallel to the dykes of Set 3 (Huang 1987).

The thickness of all the 107 dykes was measured as

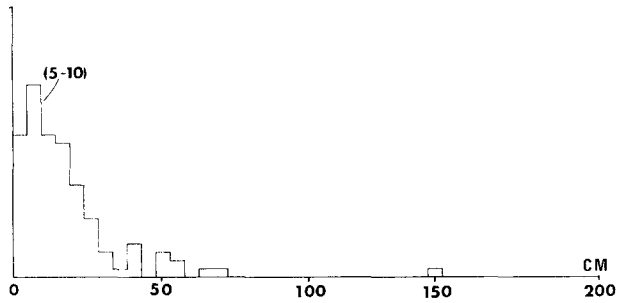

Fig. 8. Frequency histogram of dyke thicknesses classified in 5 cm intervals.

near to the turbidite beds as possible (Fig. 8). The main aim of statistical analyses on the thickness of dykes is to clarify the relationship between orientation and thickness of the dykes. Figure 8 shows the dyke planes classed in given intervals of thickness. It is easy to see that Set 1 is essentially composed of thin dykes (within 0–10 and 10–20 cm, Fig. 9a & b), the dykes of Set 2 are thicker than 10 cm (Fig. 9b & c), and the thickness of dykes in Set 3 is either within the range 0–10 cm or greater than 20 cm (Fig. 9a & c). Reasonably, dykes with small but stable thickness may be related to shear fractures, since such fractures have small width and smooth surfaces,

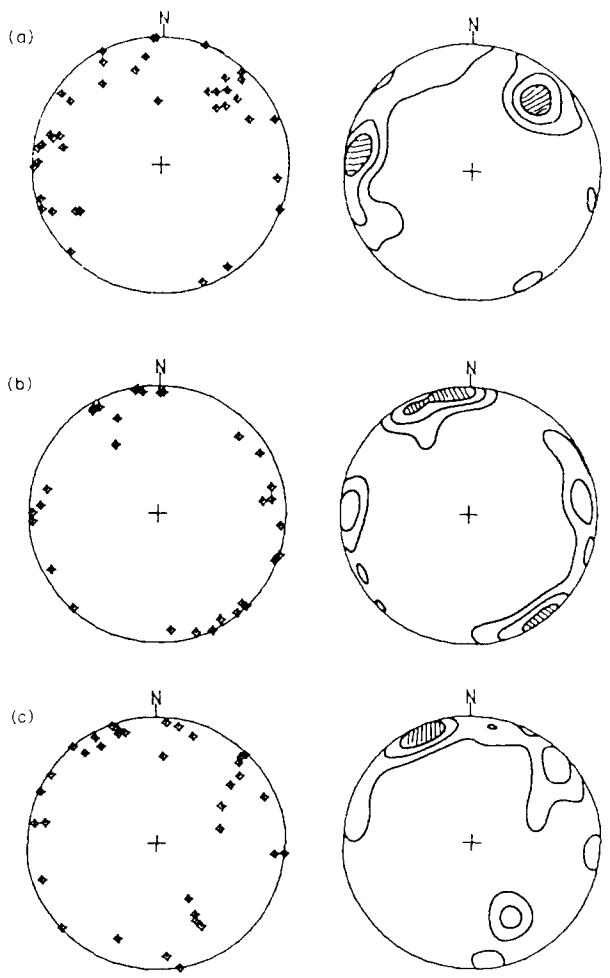

Fig. 9. Classification of dykes by their thickness (legend as in Fig. 4 for fabric diagrams). Orientation of dykes with thickness (a) less than 10 cm, (b) between 10 and 20 cm and (c) greater than 20 cm.

whereas others can be related to tension fractures which have great and variable width and rough surfaces. Based on this reasoning, the dykes of Sets 1 and 2 may have some relation with shear fractures, and those of Set 3 may be associated with tension fractures.

BIFURCATION AND BRANCHING OF DYKES: AN INDICATOR FOR DETECTING THE SENSE OF SHEAR ALONG FRACTURES

Sedimentary dykes are fossilized fractures: that is the fundamental hypothesis when studying the tectonic significance of dyke systems. Thus, a detailed mapping of branches and bifurcations around principal trunk of dykes can show the organization of the fractures, thus providing a good guide for recognizing the sense of shear of fractures. Some vertical surfaces (Fig. 10) reveal oblique dykes trending N130–140°E that offset the beds (Fig. 10b) and are arranged en échelon (Fig. 10a), indicating the relative motion of beds on both sides of the dykes. In Fig. 10(c), the convex form of the dyke shows that an oblique dyke has contoured a block of fault breccia. All these examples show that the fractures were normal faults formed before the sand intrusion.

On horizontal surfaces, the arrangement of dyke branches and bifurcations can also provide information on the relative motion on main fracture trunks. Generally, the main trunk is much thicker and has a more regular form than its branches and bifurcations. The geometry of connections between the main trunk and its bifurcations or branches is evidently related to the relative motion across the initial fracture. Figure 11 shows some examples in which the sense of shear along the main dykes is recognizable. Figure 11(b) is a map of the tail of a N068°E oriented dyke showing organization of branches; such arrangement of dyke branches could be simply explained by sinistral shear along the main trunk. The dyke bifurcations in Fig. 11(a) form a diamond-shaped figure that can also be interpreted as a result of sinistral shear along the main trunk. In contrast, in Fig. 11(c) the main trunk (trending N008°E) and its bifurcations illustrate a dextral fracture system. A typical en échelon fracture system shows that a compressional stress pattern with maximum stress trending N030–040°E may be responsible for the formation of two sets of dykes mapped in Fig. 11(d). As the two sets of dykes are vertical, this compression is horizontal. Under this compression, vertical conjugate strike-slip faults may be generated in which the dextral faults and the sinistral faults trend nearly N–S and N070–080°E, respectively (Fig. 7). Such faults have been clearly identified in Aptian limestone strata and used for determining stress states (Huang 1987).

From observations of the arrangement of main dykes and their branches and bifurcations, the dykes of Set 1 may be reasonably associated with dextral shear fractures and those of Set 2 are associated with sinistral fractures. The two sets of dykes are vertical and do not offset any beds, whereas the dykes of Set 3 have pene-

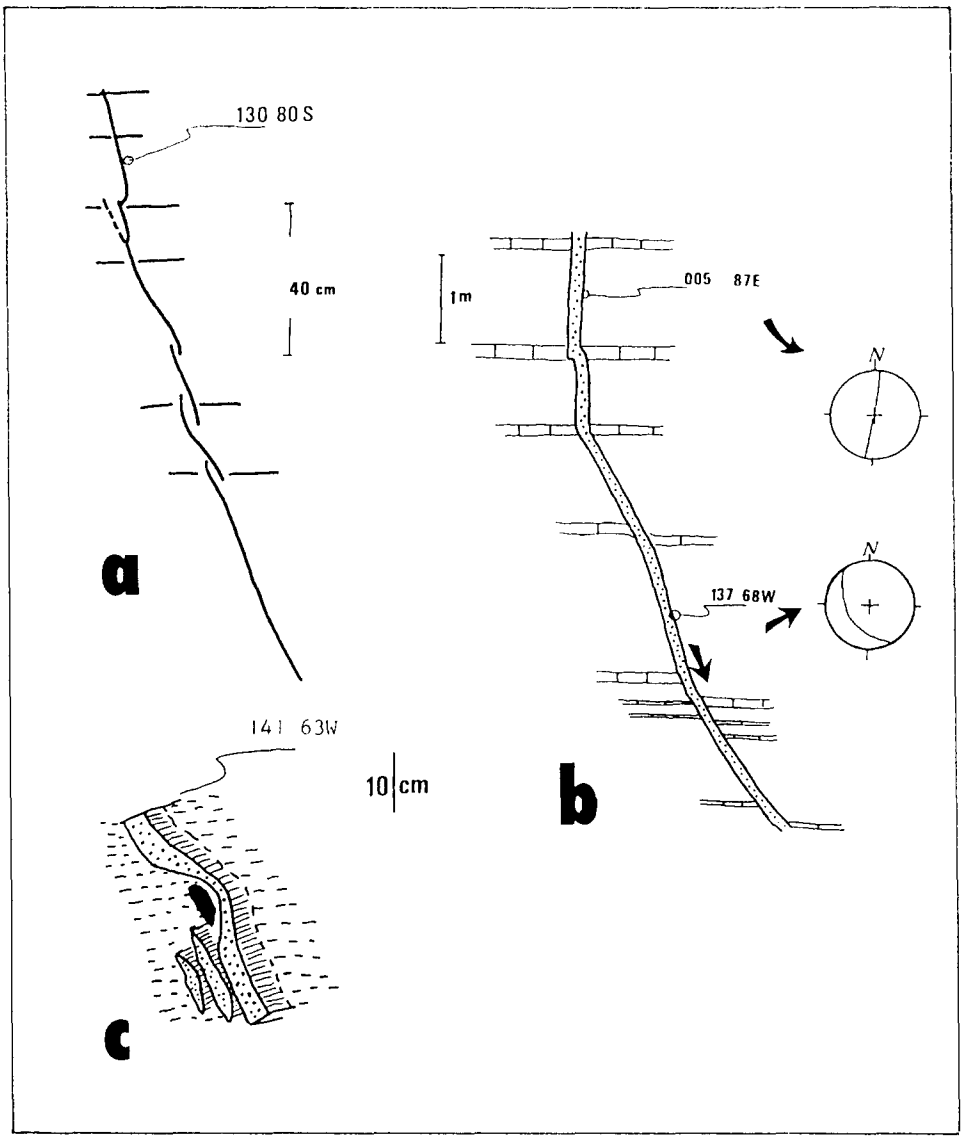

Fig. 10. Cross-sections of dykes near Bevons in early Albian strata. 141 63W indicates the strike, dip and dip direction of the dyke. The dykes are associated with Set 3.

trated normal faults with little vertical displacement of beds in some cases. From a dynamic point of view, Set 1 and Set 2 are statistically two sets of vertical conjugate fractures indicating a compressional direction along their bisecting line (N030–040°E). This hypothesis is confirmed by observations shown in Figs. 11(d) and 12. Set 3 is associated with a normal faulting activity during the late Aptian. From Fig. 10(a), one can note that the normal faults ceased their activity before the arrival of the turbidite, and thus these faults may be syn-sedimentary because the offsets on faults (Fig. 10b) decrease and die upwards in early Albian strata.

Using the method proposed by Huang & Angelier (1987), analysis of slip data on fault populations in the vicinity revealed the existence of a compatible compressional stress pattern in the Neocomian terrane as shown in Fig. 7, but no clear evidence has been found to demonstrate the existence of syn-sedimentary faulting activity during the Middle Albian by simple analysis of fault slip data. Moreover, it was difficult to quantify the horizontal displacement of the conjugate fracture system associated with the dykes of Sets 1 and 2 (Huang 1987).

DISCUSSIONS AND CONCLUSIONS

In the Sisteron region of complex Tertiary and Quaternary deformation, early faulting tectonic events are largely masked and very difficult to analyze (Huang 1987). Analyses of sedimentary dyke systems provide a useful tool for reconstructing the stress pattern under which fracture systems are generated and later used by the sand intrusions. It is clear that such analyses need many mathematic tools; statistical methods for the analysis of orientation data such as dyke planes and cluster separation, for example. Such analyses can also offer a good guide for detecting the spatial distribution of dyke planes and their geometrical characteristics.

In the case of the Sisteron area, statistical analyses of geometrical characteristics are directed mainly at verifying the perpendicularity of dyke planes with respect to bedding. Special attention was paid to the distinction of initial orientation of a dyke and late deformation, because the dykes have been folded by late compaction as well as tectonic deformation. A significant orientation datum of a dyke is its mean space orientation rather than

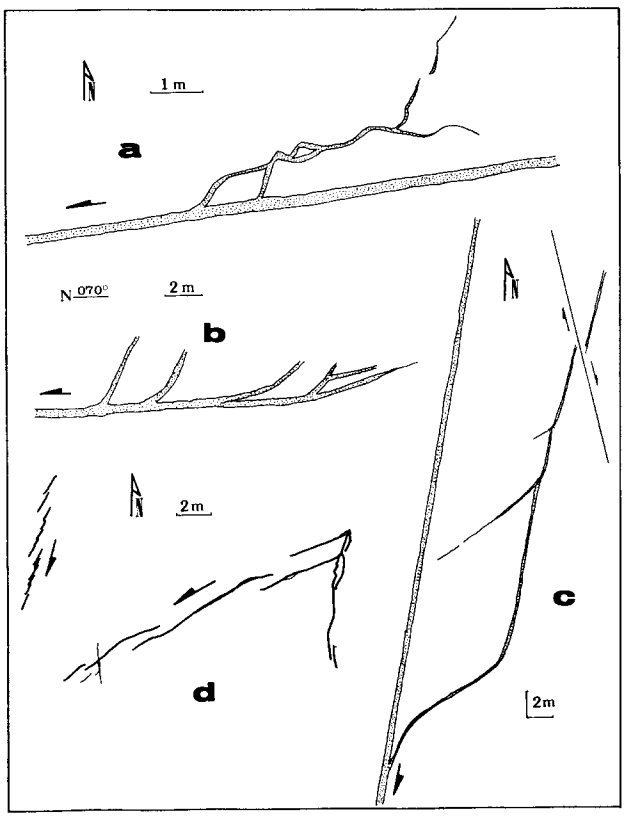

Fig. 11. Map view of dykes. (a) Dyke with bifurcation indicates the sinistral sense of shear along the fracture; (b) and (c) dykes with their branches show a sinistral (b) and dextral (c) shear senses of the initial fractures; (d) en échelon dykes indicate a conjugate fracture system compatible with a compression direction near N040°E. (a)–(c) Near Pierre-Avon in early Albian strata, (d) near le Puy in early Albian strata.

local measurements. Based on these mean space orientation data we can make a reliable statistical analysis about the orientations of fracture systems actually filled with sand. In contrast to other examples, the clastic dyke system in the Sisteron area has used several sets of fractures produced by different faulting mechanisms. Thus, to study separately the dynamic properties of fractures in each set, a cluster analysis (separation of three sets) has been made. Spatial variations in orientation of each set have been determined so that one can reasonably associate natural observations on the arrangement of bifurcations and branches of a single dyke to its related set.

Highlighted by statistical analyses, natural observations on bifurcations and branches of dykes help one to understand senses of shear along main fractures within a set of dykes. Some special arrangements of dyke bifurcations and branches are crucial for understanding dynamic features of the fractures. Certain types can be considered as important shear sense indicators: (1) branches in the tail of a dyke (Fig. 11b); (2) the form of bifurcation of dyke such as the diamond-shaped dyke in Fig. 11(a); (3) en échelon dykes (Figs. 11d and 12); (4) tension joints form (Fig. 12); (5) offset of beds in vertical section (Fig. 10b). Such information can only be acquired by detailed mapping of the dykes and their bifurcations or branches, in both vertical and horizontal sections.

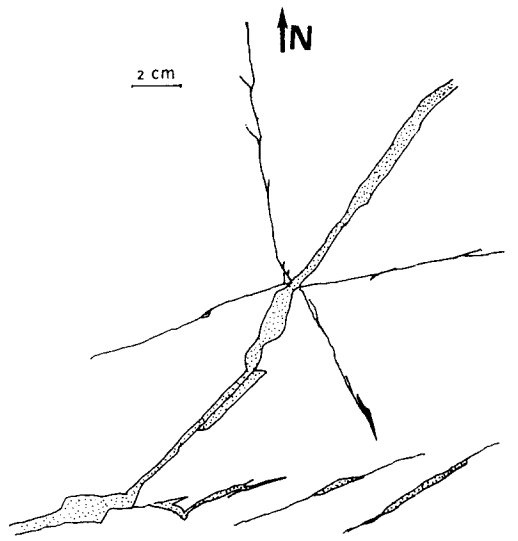

Fig. 12. Dyke fills tension joints and en échelon fracture system. Compatible compression direction is about N048°E (near le Baume in early Albian strata).

As shown by Fries (1986), the sand source of the turbidite in the Sisteron area came from the south in the Middle Albian. The intrusion of sandstone occurred surely after the Middle Albian, as the turbidite source must have been buried under sediments before penetrating into fractures (Newson 1903, Truswell 1972, Hiscott 1979). According to dynamic analyses of dykes in the Sisteron area, two important tectonic events can be recognized at that time.

(1) Before or during the early Albian, a probable normal faulting tectonic regime dominated the Sisteron area. A population of normal faults and joints trending about N135°E is partly filled by sandstone. Were these fractures due to regional tectonic deformation or related to gravitational gliding? As the orientation of the dykes of Set 3 is rather consistent and some faults parallel to the dykes have been observed in the strata of late Aptian, and the slumping activity died out gradually during the Albian (Huang 1987), it seems that these normal faults are most probably due to an extensional tectonic event with corresponding direction of extension about N030–040°E. In any case, this activity is synsedimentary because this faulting activity ceased during the early Albian (Fig. 10b).

(2) In the late Albian, the Sisteron area was submitted to a compressional tectonic regime with the principal compression direction near N030–040°E. Under this stress state, a system of conjugate joints and strike-slip faults was produced; and two sets of dykes have partly used these fractures. Faults with slip lineation are observable over the whole region, and two major sets of conjugate faults are parallel to the two sets of dykes. Analyses of a large number of these faults show a compatible stress pattern (Fig. 7). Without any sign of ductile deformation, this tectonic episode was purely brittle (Huang 1987).

Acknowledgements—This work was financially supported by the CNRS, Gis GENEBASS of France and the Government of the

People's Republic of China within the framework of Sino-French co-operation. The author thanks Professor B. Beaudoin, Professor J. Angelier and Dr C. Grandjacquet for their help with the fieldwork and with mathematical analyses in laboratory. The author also acknowledges the Associate Editor of the Journal and two anonymous referees for their constructive remarks, which enabled the manuscript to be substantially improved.

REFERENCES

Beaudoin, B. & Fries, G. 1982. Filons grèseux sédimentaires, *per descensum*, dans un système de fractures ouvertes, le cas de l'Albien de Bevons (Alpes de Haute Provence). *C. r. Acad. Sci., Paris, ser.* II, **295**, 385–387.

Beaudoin, B., Fries, G., Joseph, P. & Paternoster, B. 1983. Sills grèseux sédimentaires injectés dans l'Aptien supérieur de Rosans (Hautes Alpes). *C. r. Acad. Sci., Paris, ser.* II, **296**, 387–392.

Bergerat, F. 1987. Stress fields in the European platform at the time of Africa–Eurasia collision. *Tectonics* **6**, 99–122.

Borradaile, G. J. 1984. A short note on sandstone dyke orientations. *J. Struct. Geol.* **6**, 587–588.

Cook, A. C. & Johnson, K. R. 1970. Early joint formation in sediments. *Geol. Mag.* **110**, 361–368.

Cross, W. 1894. Intrusive sandstone dikes in granite. *Bull. geol. Soc. Am.* **5**, 225–230.

Diday, E. 1971. Une nouvelle méthode en classification automatique et reconnaissance des formes: la méthode des nuées dynamiques. *Rev. stat. Appl.* **XIX**, 2, 19–33.

Diller, J. S. 1890. Sandstone dikes. *Bull. geol. Soc. Am.* **1**, 411–442.

Duncan, J. R. 1964. Structural significance of clastic dikes in a selected exposure of the Modelo Formation, Santa Monica Mountain, California. *Bull. South. Calif. Acad. Sci.* **63**, 157–163.

Dzulynski, S. & Radomski, A. 1965. Clastic dykes in the Carpathian flysch. *Ann. Soc. geol. Pologne* **26**, 610–611.

Ferry, S. & Flandrin, J. 1979. Mégabrèche de resédimentation, lacune mécanique et pseudo-"hardground" sur la marge vocontienne au Barrémien et à l'Aptien inférieur (Sud-Est de la France). *Géol. Alpine* **55**, 75–92.

Fisher, R. A. 1953. Dispersion on a sphere. *Proc. R. Soc. Lond.* **A217**, 295–304.

Fries, G. 1986. Dynamique du bassin subalpin à l'Apto-Cénomanien. Unpublished Thesis, University of Paris VI.

Hayashi, T. 1966. Clastic dikes in Japan (I). *Jap. J. Geol. Geogr. Trans.* **37**, 1–20.

Hiscott, R. N. 1979. Clastic sills and dykes associated with deep-water sandstones. Tourelle Formation, Ordovician, Quebec. *J. Sedim. Petrol.* **49**, 1–10.

Huang, Q. 1987. Analyse géométrique et dynamique de la fracturation: application à la region de Sisteron et au Golfe de Suez. Unpublished Thesis, University of Paris VI.

Huang, Q. & Angelier, J. 1987. Les systèmes de failles conjuguées: Une méthode d'identification, de séparation et de calcul des axes de contrainte. *C. r. Acad. Sci., Paris, ser.* II, **304**, 465–468.

Huang, Q., Angelier, J. & Mechler, P. 1987. Filtrage et diagrammes d'iso-densité: un apport à l'analyse de données orientées. *C. r. Acad. Sci., Paris, ser.* II, **304**, 377–382.

Jenkins, O. P. 1952. Mechanics of clastic dike intrusion. *Engng Miner. J. Press.* **120**, 12–20.

Mardia, K. V. 1972. *Statistics of Directional Data*. Academic Press, London.

Newson, J. F. 1903. Clastic dikes. *Bull. geol. Soc. Am.* **14**, 227–268.

Pavlow, A. P. 1896. On dykes of Oligocene sandstone in the Neocomian clay of the district of Alatyr in Russia. *Geol. Mag.* **3**, 49–52.

Rutten, M. G. & Schonenberger, H. J. 1957. Syn-sedimentary sandstone dykes in the Aptian of the Serre Chaitieu, Southern France. *Geol. Mijnb.* **19**, 214–220.

Scheidegger, A. E. 1965. On the statistics of the orientation of bedding planes, grain axes and similar sedimentological data. *U.S. Geol. Survey Prof. Paper.* **525**, 164–167.

Symers, N. B. & Peterson, G. L. 1971. Sandstone dykes and sills in the Moreno shale, Panoche Hills, California. *Bull. geol. Soc. Am.* **82**, 3021–3027.

Truswell, J. F. 1972. Sandstone sheets and related intrusions from Coffee Bay, South Africa. *J. Sedim. Petrol.* **42**, 578–583.

Watson, G. S. 1960. More significant tests on the sphere. *Biometrika* **43**, 87–91.

Watson, G. S. 1965. Equatorial distribution on a sphere. *Biometrika* **52**, 193–201.

Woodcock, N. H. 1977. Specification of fabric shapes using an eigenvalue method. *Bull. geol. Soc. Am.* **88**, 1231–1236.

APPENDIX

Watson (1965) proposed a distribution for describing the orientation data on a sphere (concerning the residual magnetic directions in sedimentary rocks) that is generally called an axial distribution, with the probability density function as follows:

$$f(\theta) = C(\varkappa) \exp(-\varkappa \cos^2 \theta),$$

where

$$C(\varkappa)^{-1} = 4\pi \int_0^1 \exp(-\varkappa t^2) dt,$$

θ is the angle between the fixed point and any other points on the unit sphere. For axial distributions, $\varkappa$ is a negative parameter. For girdle distributions, $\varkappa$ is a positive parameter. The greater $\varkappa$ is, the more concentrated are the data around the fixed axis (in axial cases) or the fixed plane (for girdle cases).

For a set of data with N measurements represented by unit vectors in the Euclidian space, the orientation matrix is defined as a symmetric matrix (Watson 1965, Scheidegger 1965):

$$\boldsymbol{T} = \begin{bmatrix} \Sigma x_i^2 & \Sigma x_i y_i & \Sigma x_i z_i \\ \Sigma y_i x_i & \Sigma y_i^2 & \Sigma y_i z_i \\ \Sigma z_i x_i & \Sigma z_i y_i & \Sigma z_i^2 \end{bmatrix}.$$

From $\boldsymbol{T}$ the three eigenvalues $\lambda_1 > \lambda_2 > \lambda_3$ and their corresponding eigenvectors τ_1, τ_2 and τ_3 can be calculated. The preferred direction of this set, composed of axially distributed vectors, is estimated by the eigenvector (τ_1) corresponding to the greatest eigenvalue λ_1. The estimator of the parameter $\varkappa$ is given by the relation $C'(\varkappa)/C(\varkappa) = \lambda_1/N$ (in axial cases) or $C'(\varkappa)/C(\varkappa) = \lambda_3/N$ (in girdle cases). The values of $\varkappa$ corresponding to different λ_1/N and λ_3/N are tabulated in Mardia's book (1972).

Woodcock (1977) proposed the ratio of three eigenvalues ($\Phi = \ln(\lambda_1 - \lambda_2)/\ln(\lambda_2 - \lambda_3)$) for qualitative tests of the form of data distribution on a sphere; if $\ln(\lambda_1 - \lambda_2) = \ln(\lambda_2 - \lambda_3) = 0$, the data are uniformly distributed over the space. When the value of $\ln(\lambda_2 - \lambda_3)$ is small, the greater the value of $\ln(\lambda_1 - \lambda_2)$ and the more tightly the data concentrate around the preferred direction τ_1. When the value of $\ln(\lambda_1 - \lambda_3)$ is small the greater the value of $\ln(\lambda_2 - \lambda_3)$ and the more tightly the data concentrate about the plane with its normal represented by the vector τ_3. So the ratio Φ is a significant parameter for a qualitative estimate of the form of the data distribution.